

Sezione d'urto della fusione tra ioni pesanti con tecniche di Intelligenza Artificiale

Daniele Dell'Aquila

Dipartimento di Scienze Chimiche, Fisiche, Matematiche e Naturali, University of Sassari, Sassari, Italy

INFN – Laboratori Nazionali del Sud, Catania, Italy



uniss
UNIVERSITÀ DEGLI STUDI DI SASSARI



Complete fusion reactions: a brief overview

Nucleus-nucleus collisions at low and intermediate energies are the ideal playground to explore the evolution of reaction mechanisms with the collision energy and to probe the interplay of nuclear structure and dynamics (including the occurrence of collective motions in hot rotating nuclei).

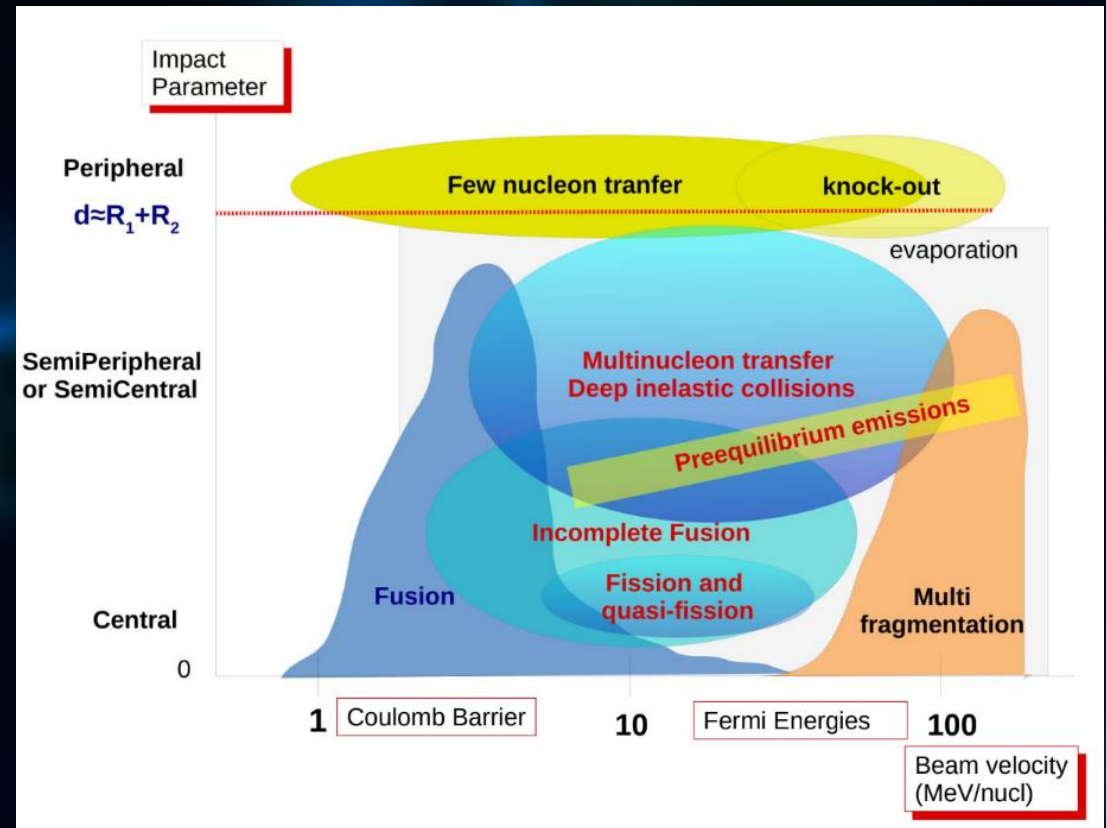
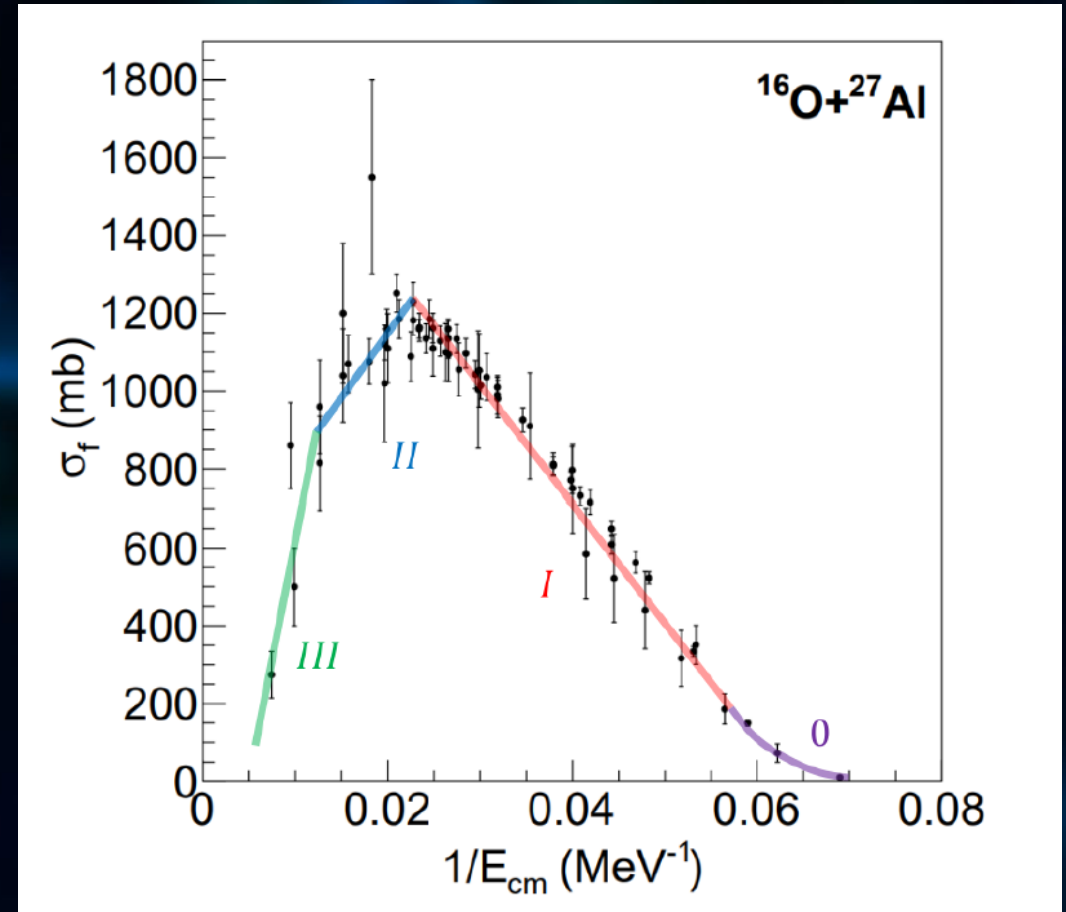


figure by Giovanni Casini (INFN-FI)

Complete fusion reactions: a brief overview

- Different, complementary, experimental methods can be effectively used to estimate the yield of evaporation residues (gamma-ray analysis, time-of-flight and magnetic spectrometers, charged particle detection with telescope arrays) → heavy-ion fusion cross section from the Coulomb barrier to the onset of multi-fragmentation →
- See e.g. *P. Frobrich, Phys. Rep. 116 (1984) 337*.



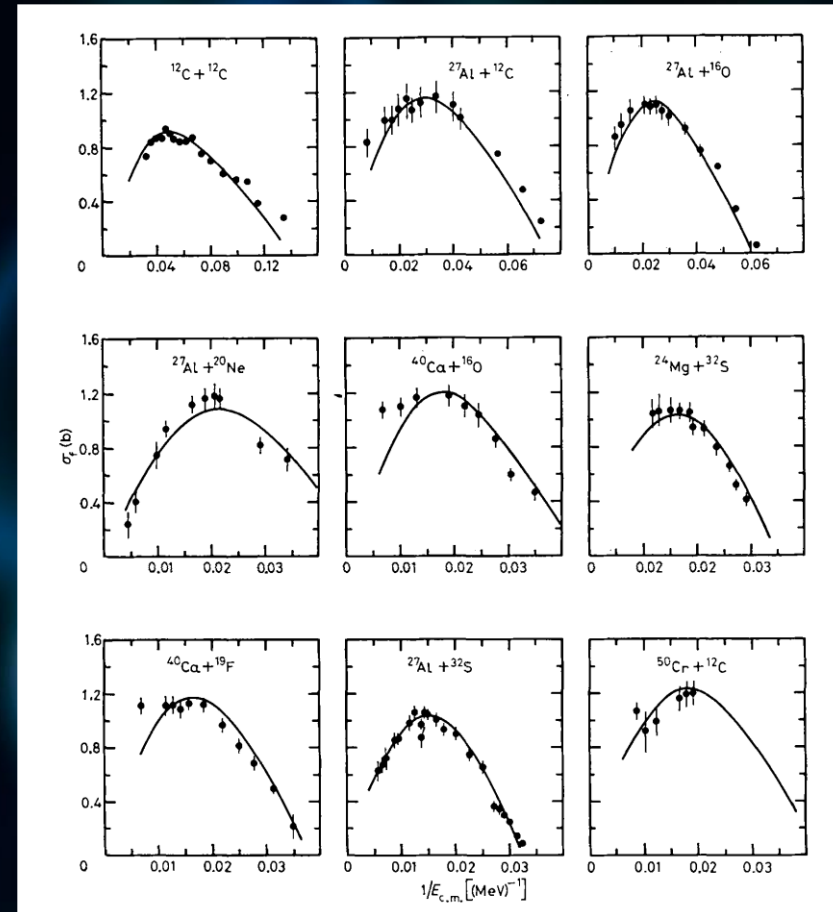
Complete fusion reactions: a brief overview

Models for the description of fusion cross section between heavy-ions:

- **Microscopical approaches:** Time-Dependent Hartree Fock (TDHF), Molecular dynamics;
- **Macroscopic models:** critical distance models, limitation to the compound nucleus model (empirical nuclear potentials from semi-classical considerations);
- **Empirical models:** starting from nuclear reaction theory and then optimizing to the experimental data.

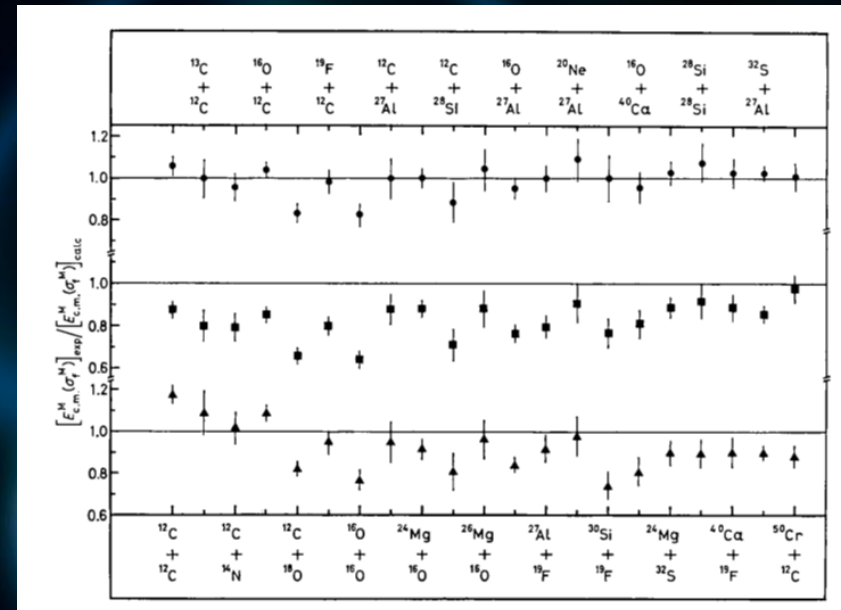
Complete fusion reactions: a brief overview

Previous data-driven
(*phenomenological*) approaches,
see e.g. **Porto F and Sambataro S
1984 Nuov. Cim. 83 339** → good
description of data around the
maxima of the cross section →
few datasets in Region III (high
energies) and Region I (close to
the Coulomb barrier).



Complete fusion reactions: a brief overview

Previous data-driven
(*phenomenological*) approaches,
see e.g. **Porto F and Sambataro S
1984 Nuov. Cim. 83 339** → good
description of data around the
maxima of the cross section →
few datasets in Region III (high
energies) and Region I (close to
the Coulomb barrier).

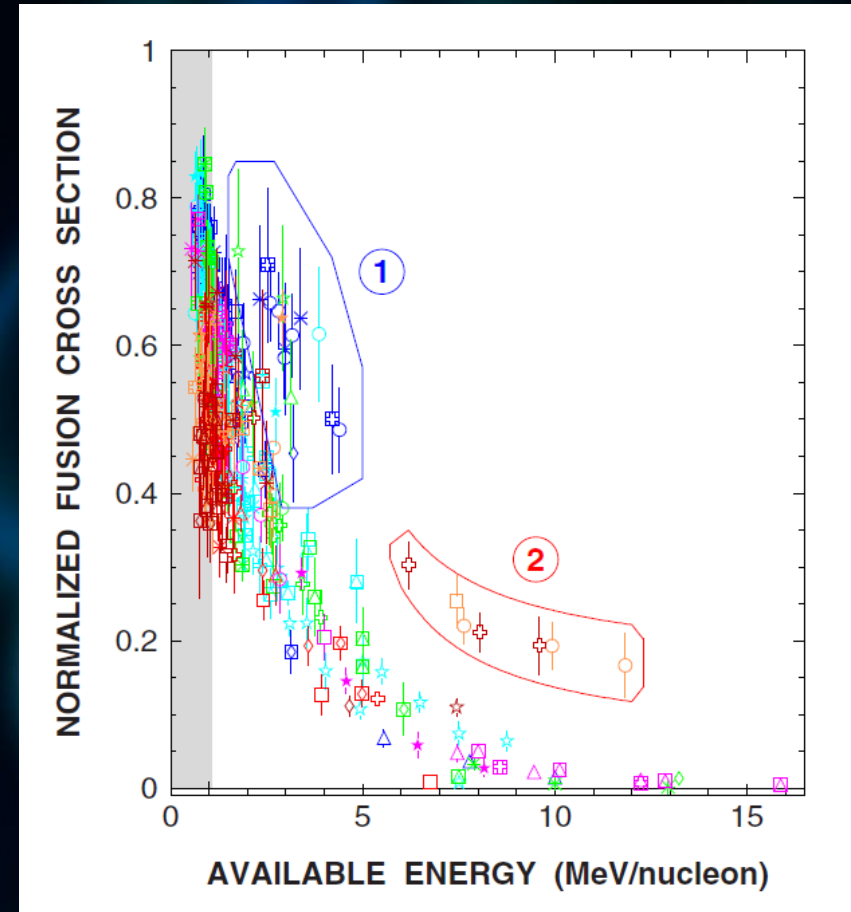


Complete fusion reactions: a brief overview

More recently → systematic study of Region III shows discrepancies for some of the systems → further investigation on both experiment and theory is required!

Fusion cross section in Region III → disagreement with the prediction of state-of-the-art for some collision systems such as:

- $^{28}\text{Si}+^{12}\text{C}$
- $^{12}\text{C}+^{27}\text{Al}$
- $^{48}\text{Ti}+^{40}\text{Ca}$
- $^{16}\text{O}+^{40}\text{Ca}$
- $^{14}\text{N}+^{12}\text{C}$
- $^{14}\text{N}+^{14}\text{N}$
- $^{14}\text{N}+^{27}\text{Al}$
- $^{14}\text{N}+^{52}\text{Cr}$
- $^{14}\text{N}+^{58}\text{Ni}$



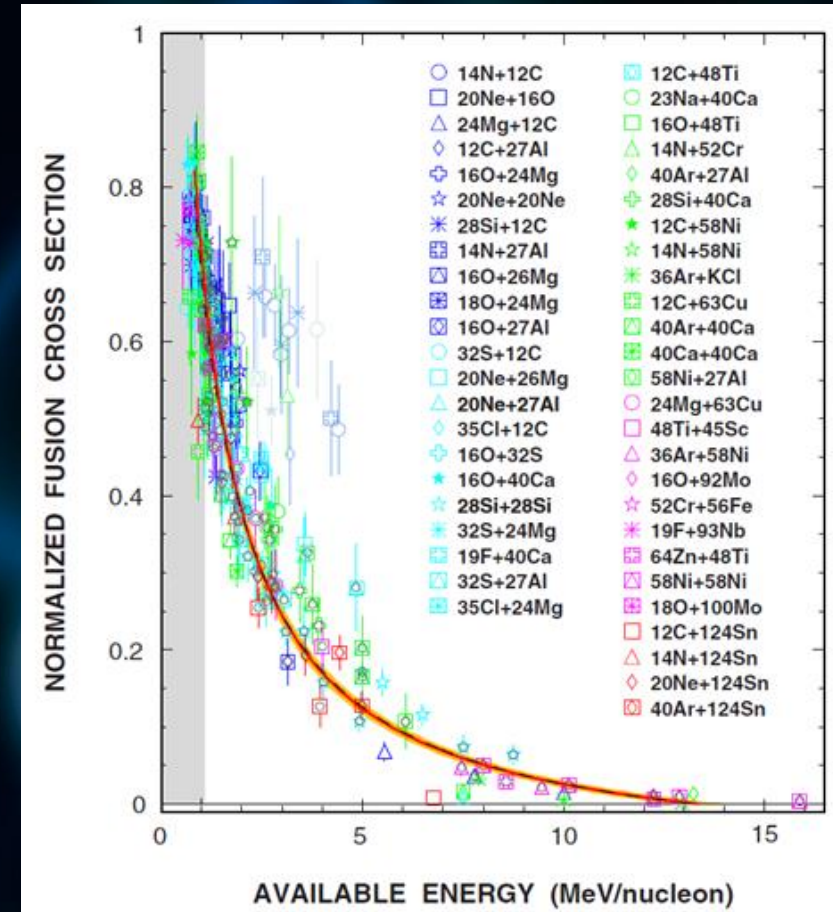
from P. Eudes et al., Phys. Rev. C 90 (2014) 034609.

Complete fusion reactions: a brief overview

More recently → systematic study of Region III shows discrepancies for some of the systems → further investigation on both experiment and theory is required!

Fusion cross section in Region III → disagreement with the prediction of state-of-the-art for some collision systems such as:

- $^{28}\text{Si}+^{12}\text{C}$
- $^{12}\text{C}+^{27}\text{Al}$
- $^{48}\text{Ti}+^{40}\text{Ca}$
- $^{16}\text{O}+^{40}\text{Ca}$
- $^{14}\text{N}+^{12}\text{C}$
- $^{14}\text{N}+^{14}\text{N}$
- $^{14}\text{N}+^{27}\text{Al}$
- $^{14}\text{N}+^{52}\text{Cr}$
- $^{14}\text{N}+^{58}\text{Ni}$



from P. Eudes et al., Phys. Rev. C 90 (2014) 034609.

Approach, dataset, and modeling

About 50 years of systematics (see e.g. *Nuclear Reactions Video: Karpov A et al., 2017 Nucl. Instrum. Meth. Phys. Res. A 859 112; Zagrebaev V et al., 1999 NRV web knowledge base on low-energy nuclear physics URL <http://nrw.jinr.ru/> for a complete database) → Possibility to derive new **data-driven** models for the description of the fusion cross section between heavy-ions in Regions I-III.*

Experimental data on HI fusion cross sections		
Experimental data on fusion elastic scattering evaporation residue	Specify fusion reaction (at least one item) Z_1 <input type="text"/> A_1 <input type="text"/> + Z_2 <input type="text"/> A_2 <input type="text"/> Search or choose it from the list <input type="text"/> Go	(Quite recently we started to fill the database. We are very far from finish...) Show all accumulated data
Ordered by P-T combination, ascending nucleus , time of publication		
(access to the source may be restricted by owner)		
$^4\text{He} + ^{48}\text{Ni} \rightarrow ^{52}\text{Zn}$ (EiR)	E.F. Aguilera, E. Martinez-Quiroz, R. Chavez-Gonzalez et al.,	Physical Review, C 87 (2013) 14613
$^4\text{He} + ^{107}\text{Er} \rightarrow ^{111}\text{Yb}$ (EiR)	S. Gil, R. Vandenbosch, A. Charlop et al.,	Physical Review, C 43 (1991) 701
$^4\text{He} + ^{181}\text{Ta} \rightarrow ^{185}\text{Re}$ (FF)	F. D. Becchetti, K. H. Hicks, C. A. Fields et al.,	Physical Review, C 28 (1983) 1217
$^4\text{He} + ^{197}\text{Au} \rightarrow ^{201}\text{Tl}$ (FF)	F. D. Becchetti, K. H. Hicks, C. A. Fields et al.,	Physical Review, C 28 (1983) 1217
$^4\text{He} + ^{209}\text{Bi} \rightarrow ^{213}\text{At}$ (FF)	F. D. Becchetti, K. H. Hicks, C. A. Fields et al.,	Physical Review, C 28 (1983) 1217
$^4\text{He} + ^{215}\text{Tl} \rightarrow ^{219}\text{U}$ (FF)	F. D. Becchetti, K. H. Hicks, C. A. Fields et al.,	Physical Review, C 28 (1983) 1217
$^4\text{He} + ^{40}\text{Ca} \rightarrow ^{44}\text{Ti}$ (EiR)	K.A. Eberhard, Ch. Appel, R. Bangert et al.,	Physical Review Letters, 43 (1979) 107
$^4\text{He} + ^{44}\text{Ca} \rightarrow ^{48}\text{Ti}$ (EiR)	K.A. Eberhard, Ch. Appel, R. Bangert et al.,	Physical Review Letters, 43 (1979) 107
$^4\text{He} + ^{63}\text{Cu} \rightarrow ^{67}\text{Ga}$ (EiR)	A. Navin, V. Tripathi, Y. Blumenfeld et al.,	Physical Review, C 70 (2004) 44601
$^4\text{He} + ^{65}\text{Cu} \rightarrow ^{69}\text{Ga}$ (EiR)	A. Navin, V. Tripathi, Y. Blumenfeld et al.,	Physical Review, C 70 (2004) 44601
$^4\text{He} + ^{67}\text{Zn} \rightarrow ^{71}\text{Ge}$ (X-rays from EC of EiR)	M. Fischella, V. Scuderi, A. Di Pietro et al.,	Journal of Physics, 282 (2011) 012014
$^4\text{He} + ^{70}\text{Zn} \rightarrow ^{74}\text{Ge}$ (EiR)	V. Scuderi, A. Di Pietro, P. Figueroa et al.,	Physical Review, C 84 (2011) 64604
$^4\text{He} + ^{72}\text{Zn} \rightarrow ^{76}\text{Ge}$ (EiR)	A. Di Pietro, P. Figueroa, V. Scuderi et al.,	Physics of Atomic Nuclei, 69 (2006) 1366
$^4\text{He} + ^{92}\text{Nb} \rightarrow ^{96}\text{Tb}$ (EiR)	C. S. Palshekar, S. Santra, A. Chatterjee, K. Ramachandran, Shital Tha,	Physical Review, C 82 (2010) 044608
$^4\text{He} + ^{107}\text{Ag} \rightarrow ^{111}\text{In}$ (FF)	A. Butkevitz, H. H. Duhm, F. Goldenbaum et al.,	Physical Review, C 60 (2009) 37603
$^4\text{He} + ^{136}\text{La} \rightarrow ^{140}\text{Pr}$ (FF)	A. Butkevitz, H. H. Duhm, F. Goldenbaum et al.,	Physical Review, C 60 (2009) 37603
$^4\text{He} + ^{160}\text{Dy} \rightarrow ^{164}\text{Er}$ (EiR)	S. Gil, R. Vandenbosch, A. J. Lazzarini et al.,	Physical Review, C 31 (1985) 1752
$^4\text{He} + ^{164}\text{Ho} \rightarrow ^{168}\text{Tm}$ (FF)	R. Broda, M. Ishihara, B. Herskind et al.,	Nuclear Physics, A 248 (1975) 356
$^4\text{He} + ^{166}\text{Er} \rightarrow ^{170}\text{Yb}$ (EiR)	A. Butkevitz, H. H. Duhm, F. Goldenbaum et al.,	Physical Review, C 60 (2009) 37603
$^4\text{He} + ^{180}\text{Os} \rightarrow ^{184}\text{Pt}$ (EiR)	S. Gil, R. Vandenbosch, A. Charlop et al.,	Physical Review, C 43 (1991) 701
$^4\text{He} + ^{186}\text{Os} \rightarrow ^{190}\text{Pt}$ (EiR)	A. Navin, V. Tripathi, Y. Blumenfeld et al.,	Physical Review, C 70 (2004) 44601
$^4\text{He} + ^{197}\text{Au} \rightarrow ^{201}\text{Tl}$ (FF)	D. L. Uhl, T. L. McDaniel, J. W. Cobble,	Physical Review, C 4 (1971) 1357
$^4\text{He} + ^{199}\text{Au} \rightarrow ^{203}\text{Tl}$ (FF)	J. Ralarosy, M. Debeauvais, G. Remy et al.,	Physical Review, C 8 (1973) 2372
$^4\text{He} + ^{201}\text{Au} \rightarrow ^{205}\text{Tl}$ (FF)	J. Gindler, H. Munzel, J. Buschmann et al.,	Nuclear Physics, A 145 (1970) 337
$^4\text{He} + ^{203}\text{Au} \rightarrow ^{207}\text{Tl}$ (EiR)	H. E. Kutz, E. W. Jasper, K. Fischer et al.,	Nuclear Physics, A 168 (1971) 129
$^4\text{He} + ^{205}\text{Au} \rightarrow ^{209}\text{Tl}$ (FF)	A. Butkevitz, H. H. Duhm, F. Goldenbaum et al.,	Physical Review, C 60 (2009) 37603
$^4\text{He} + ^{207}\text{Au} \rightarrow ^{211}\text{Tl}$ (FF)	J.R. Huizenga, R. Chaudhry, R. Vandenbosch,	Physical Review, 126 (1962) 210
$^4\text{He} + ^{209}\text{Au} \rightarrow ^{213}\text{Bi}$ (FF)	J.R. Huizenga, R. Chaudhry, R. Vandenbosch,	Physical Review, 126 (1962) 210
$^4\text{He} + ^{211}\text{Bi} \rightarrow ^{215}\text{Po}$ (FF)	J.R. Huizenga, R. Chaudhry, R. Vandenbosch,	Physical Review, 126 (1962) 210
$^4\text{He} + ^{213}\text{Po} \rightarrow ^{217}\text{Po}$ (FF)	J. Ralarosy, M. Debeauvais, G. Remy et al.,	Physical Review, C 8 (1973) 2372
$^4\text{He} + ^{215}\text{Po} \rightarrow ^{219}\text{Po}$ (FF)	S.M. Lukyanov, Yu.E. Penionzhkevich, R.A. Astabatie et al.,	Physics Letters, B 670 (2009) 321
$^4\text{He} + ^{217}\text{Po} \rightarrow ^{221}\text{At}$ (FF)	W. G. Meyer, V. E. Viola, Jr., R. G. Clark et al.,	Physical Review, C 20 (1979) 1716
$^4\text{He} + ^{219}\text{At} \rightarrow ^{223}\text{At}$ (FF)	D. L. Uhl, T. L. McDaniel, J. W. Cobble,	Physical Review, C 4 (1971) 1357
$^4\text{He} + ^{221}\text{At} \rightarrow ^{225}\text{At}$ (FF)	J. Ralarosy, M. Debeauvais, G. Remy et al.,	Physical Review, C 8 (1973) 2372
$^4\text{He} + ^{223}\text{At} \rightarrow ^{227}\text{At}$ (FF)	Yu.E. Penionzhkevich, Yu.A. Muzychka, S.M. Lukyanov et al.,	European Physical Journal, A 13 (2002) 123
$^4\text{He} + ^{225}\text{At} \rightarrow ^{229}\text{At}$ (FF)	A. S. Fomichev, I. David, Z. Dlouhy et al.,	Zeitschrift für Physik, 361 (1995) 129
$^4\text{He} + ^{227}\text{At} \rightarrow ^{231}\text{At}$ (FF)	J. Gindler, H. Munzel, J. Buschmann et al.,	Nuclear Physics, A 145 (1970) 337
$^4\text{He} + ^{229}\text{At} \rightarrow ^{233}\text{At}$ (FF)	J.R. Huizenga, R. Chaudhry, R. Vandenbosch,	Physical Review, 126 (1962) 210
$^4\text{He} + ^{231}\text{At} \rightarrow ^{235}\text{At}$ (FF)	J. Ralarosy, M. Debeauvais, G. Remy et al.,	Physical Review, C 8 (1973) 2372
$^4\text{He} + ^{233}\text{At} \rightarrow ^{237}\text{At}$ (FF)	W. G. Meyer, V. E. Viola, Jr., R. G. Clark et al.,	Physical Review, C 20 (1979) 1716
$^4\text{He} + ^{235}\text{At} \rightarrow ^{239}\text{At}$ (FF)	H. Frieseleben, J. R. Huizenga,	Nuclear Physics, A 224 (1974) 503
$^4\text{He} + ^{237}\text{At} \rightarrow ^{241}\text{At}$ (FF)	J. Gindler, H. Munzel, J. Buschmann et al.,	Nuclear Physics, A 145 (1970) 337

Approach, dataset, and modeling

Approach: *supervised learning* using ***symbolic regression*** algorithms.

Novelties:

- Deriving mathematical expressions to describe the data → support to theories and models attempting to predict the fusion cross section between heavy-ions;
- Comprehensive analysis of large amount of nuclear data → universal model for the description of the entire dataset;
- Advanced feature selection → allows to inspect the dependence on several variables (including nuclear structure variables).

Major challenges:

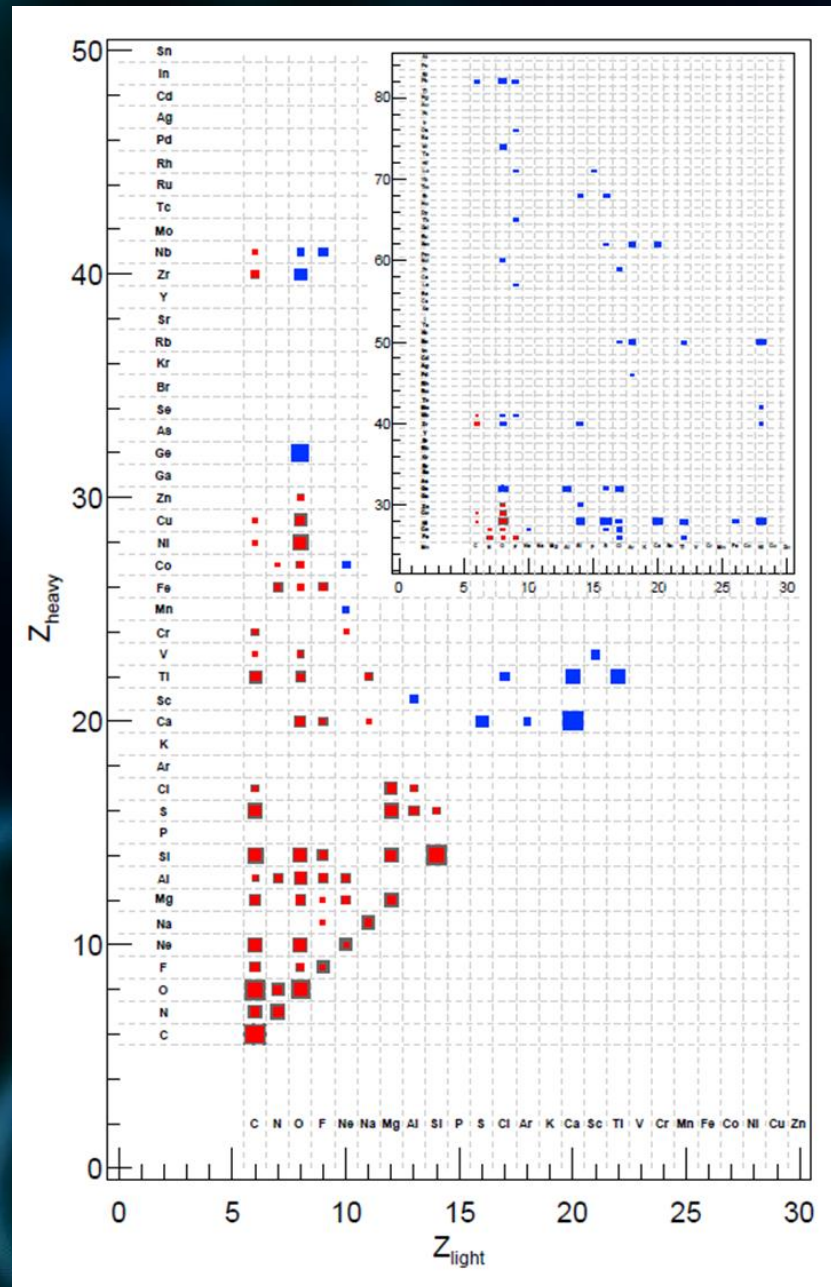
- The amplitude of the cross section varies even by several orders of magnitude with the energy;
- Experimental errors associated to each individual data point differ by several orders of magnitude for each data point;
- Resulting models must have physical boundaries and extrapolation capabilities.

We used an extensive set of *nuclear* features linked to:

- 1) The nature of the collision partners;
- 2) The energy of the collision;
- 3) The structure of the collision partners;
- 4) The structure of the compound nucleus.

Symbol	Description
E_{cm}	collision center-of-mass energy (MeV)
Z_1	charge of the first reaction partner
Z_2	charge of the second reaction partner
N_1	number of neutrons of the first reaction partner
N_2	number of neutrons of the second reaction partner
A_1	mass of the first reaction partner
A_2	mass of the second reaction partner
J_1	spin of the first reaction partner
J_2	spin of the second reaction partner
π_1	parity of the first reaction partner (1 for positive parity, -1 for negative parity)
π_2	parity of the second reaction partner (1 for positive parity, -1 for negative parity)
μ_1	magnetic dipole momentum of the first reaction partner (μ_N)
μ_2	magnetic dipole momentum of the second reaction partner (μ_N)
$\langle r^2 \rangle_1$	rms charge radius of the first reaction partner (fm)
$\langle r^2 \rangle_2$	rms charge radius of the second reaction partner (fm)
Q -value	fusion Q -value (MeV)
S_α	α separation energy of the compound nucleus (MeV)
S_n	one-neutron separation energy of the compound nucleus (MeV)
S_{2n}	two-neutron separation energy of the compound nucleus (MeV)
S_p	one-proton separation energy of the compound nucleus (MeV)
S_{2p}	two-proton separation energy of the compound nucleus (MeV)
$S_{\alpha 1}$	α separation energy of the first reaction partner
$S_{\alpha 2}$	α separation energy of the second reaction partner
S_{n1}	one-neutron separation energy of the first reaction partner
S_{n2}	one-neutron separation energy of the second reaction partner
S_{p1}	one-proton separation energy of the first reaction partner
S_{p2}	one-proton separation energy of the second reaction partner
S_{2n1}	two-neutron separation energy of the first reaction partner
S_{2n2}	two-neutron separation energy of the second reaction partner
S_{2p1}	two-proton separation energy of the first reaction partner
S_{2p2}	two-proton separation energy of the second reaction partner

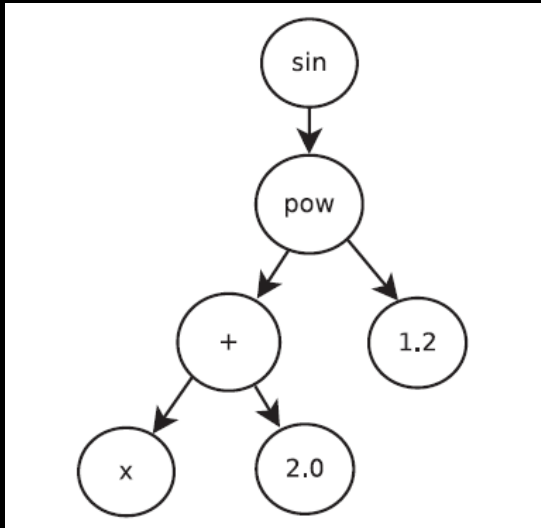
- Dataset used for model derivation → about 4500 experimental data points.
- Learning dataset: $Z_p Z_t < 250$ → light-to-medium mass nuclei.
- Testing dataset 1: $Z_p Z_t \geq 250$ → heavy systems (test the extrapolation towards heavy systems).
- Testing dataset 2: $Z_p Z_t < 250$ → some of the lighter systems.



The Brain Project

Brain Project – a neural-genetic tool for the formal modeling of data

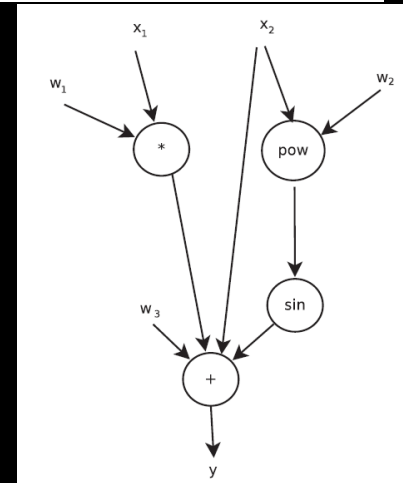
Exploits a novel hybridization of genetic programming and artificial neural network → the task is that of symbolic regression. Genetic part → foresees the evolution of tree-like structures representing mathematical expressions → deals with the global search for the maximum of a suitable fitness function; Neural part → deals with the local search for the minimum of the error when the genetic part has identified a good maximum of the fitness function.



Genetic evolution of tree-like structures representing mathematical expressions

+

$$y = 2.5 * x_1 + \sin(x_2^{3.8}) + x_2 + 1.5$$



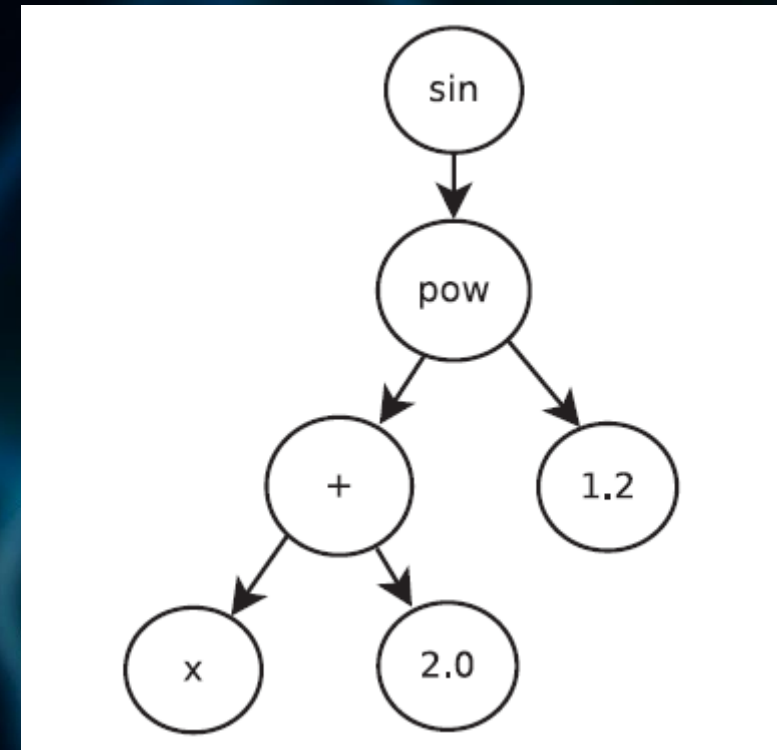
Artificial neural networks to optimize the constants (gradient descent technique)

*Russo M 2016 Swarm Evo. Comput. 27 145
Russo M 2020 Soft Comput. 24 16885–16894*

The Brain Project: genetic mechanism

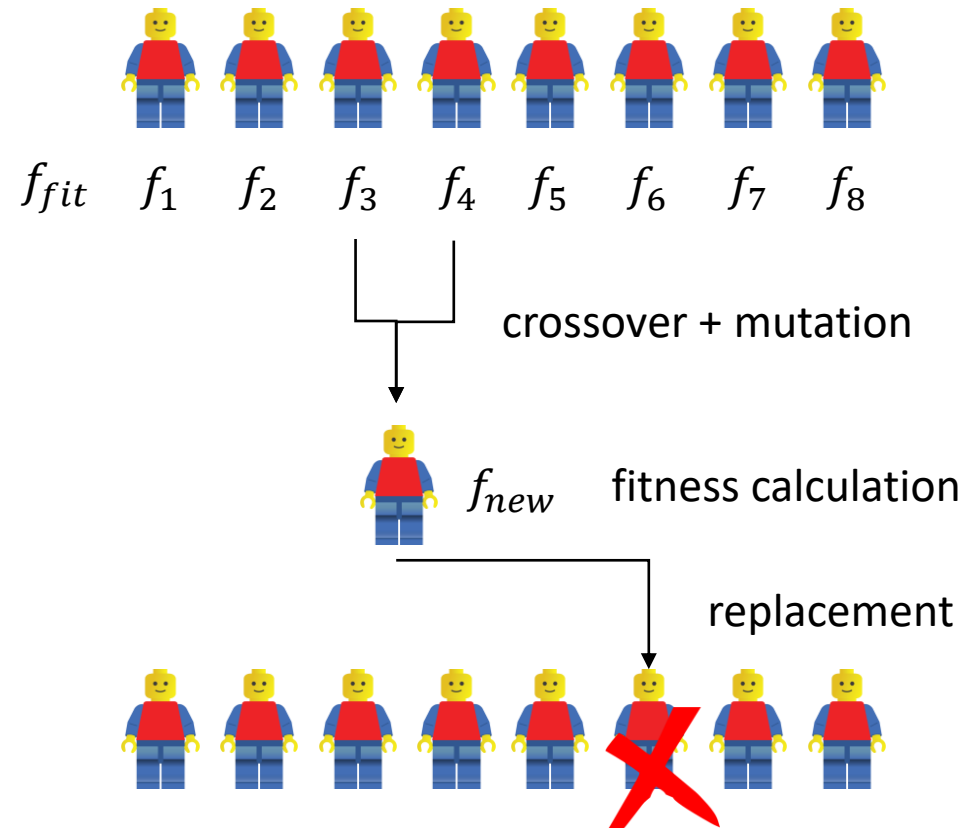
Brain Project: the genetic part forsee the evolution of tree-like structures representing mathematical expressions to model the data. In these structures, a node is a mathematical function or operation, a constant or a variable. The number of nodes is used to evaluate the complexity of the model.

→ See e.g. John R. Koza, *Genetic Programming – On the Programming of Computers by Means of Natural Selection*, A Bradford Book – The MIT Press (Cambridge, Massachusetts; London, England)

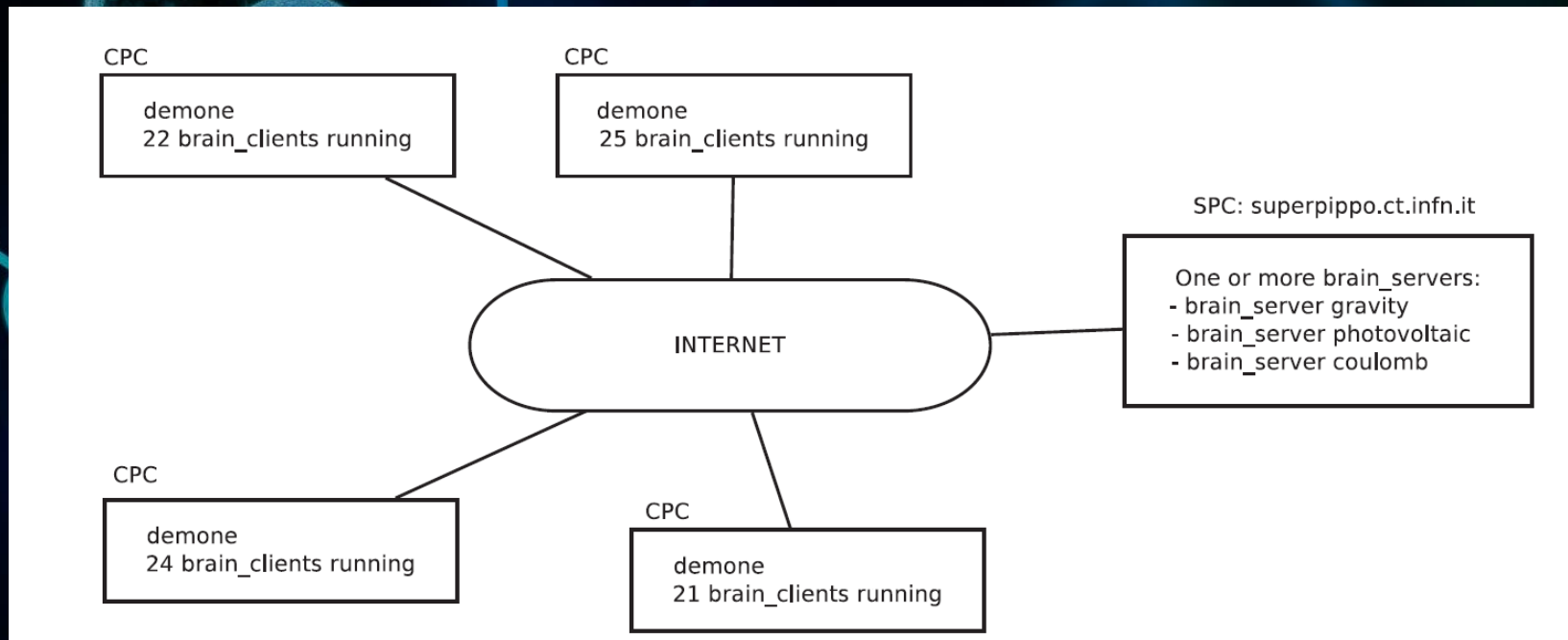


The Brain Project: genetic mechanism

1. A set of possible solutions to the optimization problem, encoded according to a predefined scheme, is generated (often randomly). Each of such solutions is called *individual*. A set of individuals forms a *population*.
2. A numerical value, called *fitness*, is associated to each individual. The fitness quantifies how much a given solution is *suitable* to the problem to solve. Generally speaking, the higher is the fitness associated to an individual the more promising is the individual itself. This is a crucial quantity for the success of the optimization procedure.
3. Until a predefined convergence criterion is reached, the following steps are iterated:
 - (a) Some individuals are selected (*parents*) to be used as a starting point for the generation of new individuals (*offsprings*).
 - (b) Offsprings are obtained through a suitable mechanism of parents encoding recombination (*crossover*). In this phase, the chromosomes of the parents, i.e. their encoding, are suitably combined to generate new individuals. A valid crossover should produce individuals whose genetic code is, to some extent, similar to that of the parents. Crossover is usually followed by a random variation, with low probability, of some portions of the derived encoding. Such a process is called *mutation* and has a crucial importance as it allows to introduce missing genetic code and to keep genetic diversity in the population. The fitness is finally calculated for all newly obtained individuals.
 - (c) Some offsprings live sufficiently long to replace other pre-existing individuals.



The Brain Project: genetic mechanism



from Russo M 2016 Swarm Evo. Comput. 27 145

The Brain Project: fitness function

Fitness function → is the function to maximize → it suitably contains the prediction error and a term related to the complexity of the model and/or feature costs.

to tune the desired trade-off between accuracy and complexity

$$f_{\text{fit}} = 100.0 * \frac{f_e u(f_e) + \alpha f_n u(f_n)}{1 + \alpha} e^{f_e(1 - u(f_e))} e^{f_n(1 - u(f_n))}$$

$$f_e = \frac{e_{\text{max}} - e}{e_{\text{max}}}$$

related to the accuracy of the model

$$e = 100 \sqrt{\sum_{o=1}^{N_o} \sum_{p=1}^{N_p} \frac{(w_{\text{pat}_p} w_{\text{out}_o} (y_{op}^d - y_{op}^c))^2}{N_o N p_{eq}}}$$

$$f_n = \frac{n_{\text{max}} - n}{n_{\text{max}} - 1}$$

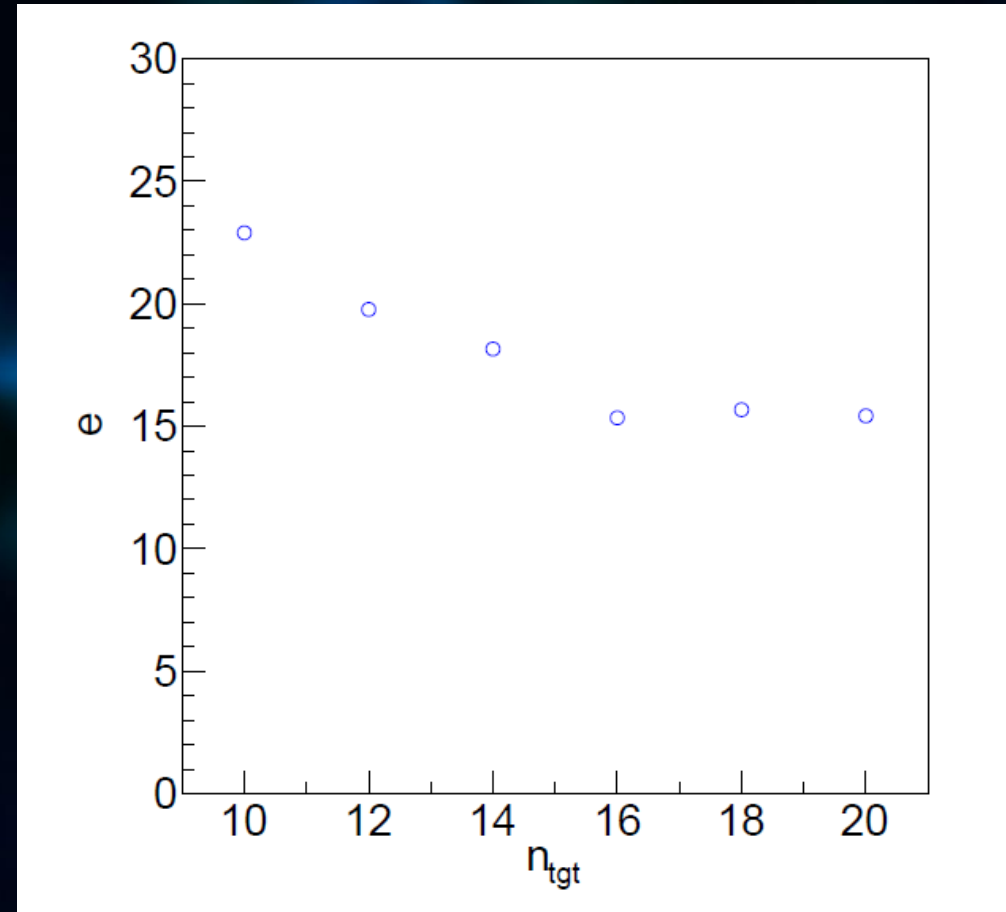
related to the complexity of the model

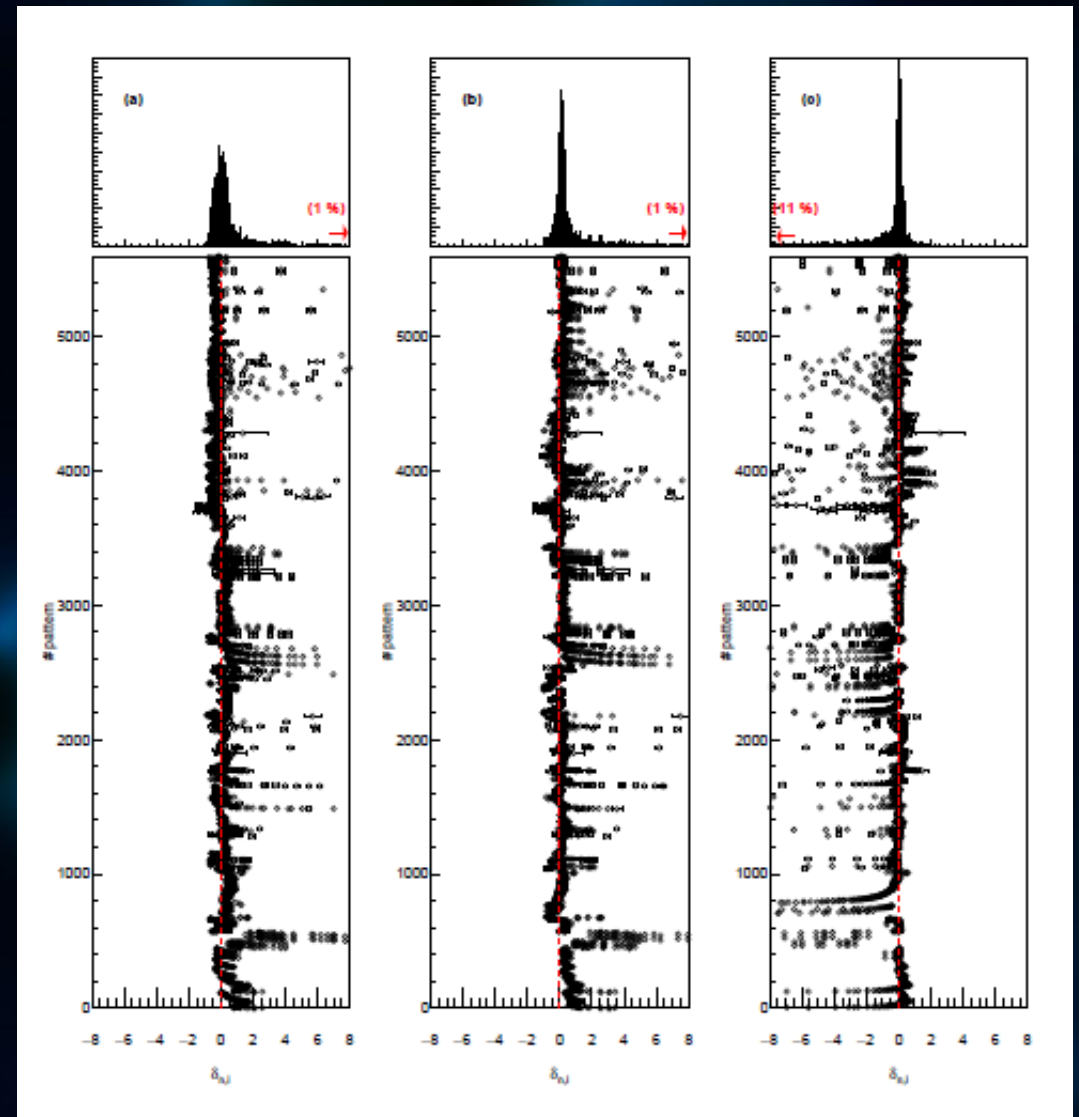
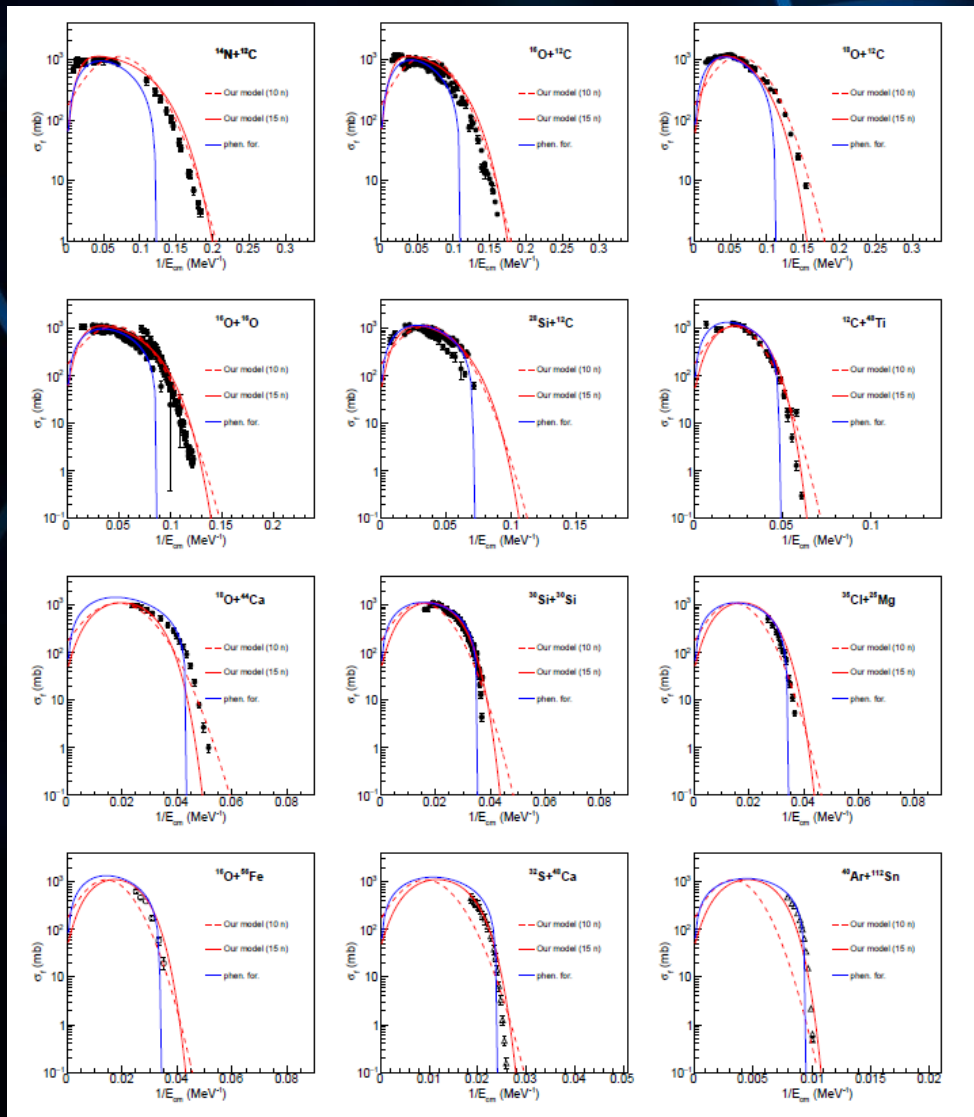
Results

$f_{fit} = f_{fit} \cdot e^{\frac{n_{tgt}-n}{n_{tgt}}}$ → required to reach a predefined, target, number of nodes. Brain Project usually tries to optimize the error with a given number of nodes → interesting to more easily tune the complexity of the desired model.

$$\sigma_{fus}^{(n_{tgt}=10)}(E_{cm}) = 1103 \cdot \exp \left[- \left(1.387 - 0.468 \cdot \frac{Z_2 \cdot Z_1}{E_{cm}} \right)^2 \right]$$

$$\sigma_{fus}^{(n_{tgt}=15)}(E_{cm}) = 1116 \cdot \exp \left[- \sinh^2 \left(-1.359 + \operatorname{erf} \left(\frac{S_{2n}}{E_{cm}} \right) + 0.061 \cdot \frac{A_1 \cdot A_2}{E_{cm}} \right) \right]$$





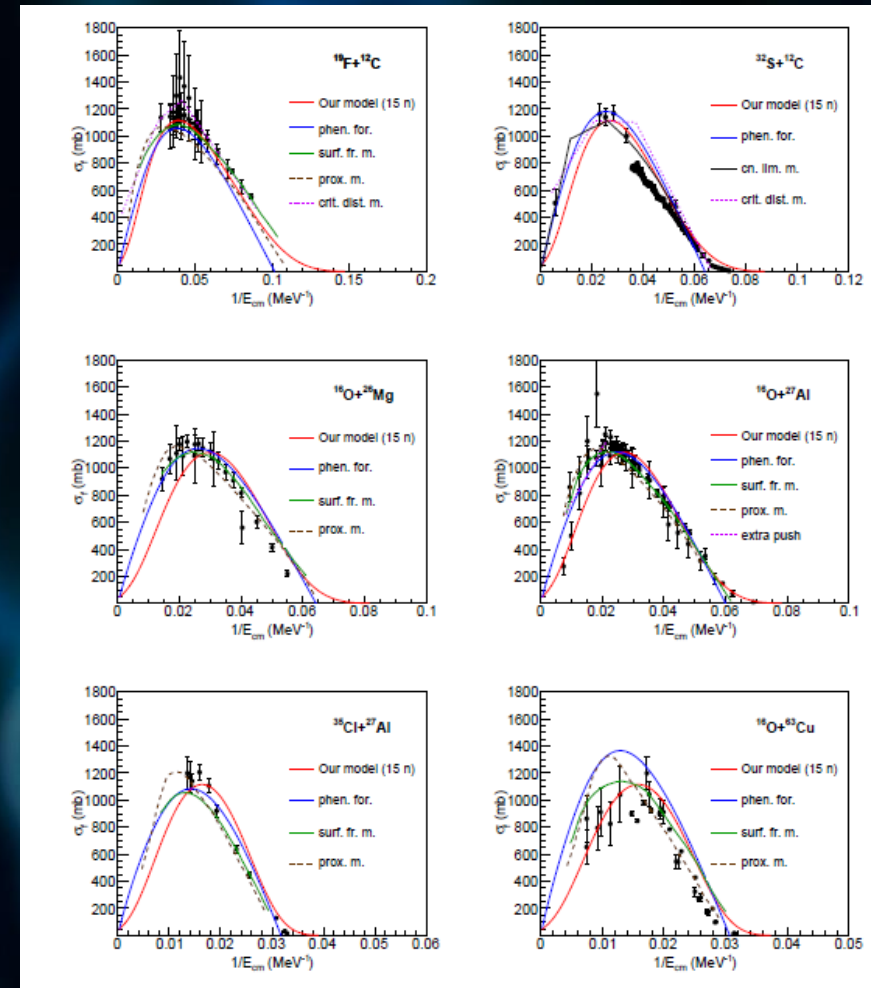
Comparison with other models


Our model slightly overestimates data in region 0;

Regions I-III → good overall description of data;

The positions of maxima are well reproduced, for lighter systems the maximum is predicted at slightly lower energies;

Nearly-symmetric systems → variances in agreement with surface friction model and slightly larger than those obtained with the proximity model.





Daniele Dell'Aquila^{2,3}, Brunilde Gnoffo¹, Ivano Lombardo^{1,4},
Francesco Porto^{3,4} and Marco Russo^{1,4}

1 INFN - Sezione di Catania, Catania, Italy

2 Dipartimento di Scienze Chimiche, Fisiche, Matematiche e Naturali, Università degli Studi di
Sassari, Sassari, Italy

3 INFN - Laboratori Nazionali del Sud, Catania, Italy

4 Dipartimento di Fisica e Astronomia, Università degli Studi di Catania, Catania,
Italy

Thank you for your attention!